Photosynthetic H2 generation and organic transformations with CdSe@CdS-Pt nanorods for highly efficient solar-to-chemical energy conversion

Photosynthetic H_2 Generation and Organic Transformations with CdSe@CdS-Pt Nanorods for Highly Efficient Solar-to-Chemical Energy Conversion

Agosti Amedeo[1], Nakibli Yifat[2], Amirav Lilac[2], Bergamini Giacomo[1*]*

[1]*Chemistry Department "Giacomo Ciamician", University of Bologna, 40129 Bologna, Italy*
[2]*Schulich Faculty of Chemistry, Technion-Israel Institute of Technology, 32000 Haifa, Israel*

Corresponding Authors' e-mail addresses:
Lilac Amirav: lilac@technion.ac.il; *Giacomo Bergamini:* giacomo.bergamini@unibo.it

Abstract

The framework of solar-to-chemical energy conversion is mapped by an exploding investigation space, aiming at rapid elevation of the technology to commercially relevant performances and processing conditions. Prospective materials and alternative oxidative pathways are revolutionizing water-splitting into decoupled hydrogen and high-value added chemicals production. Yet, pioneering solar refinery systems have been limited to either efficient, but isolated half-reactions or sluggish simultaneous red-ox transformations, hampering the forthcoming adoption of this promising solar-harvesting strategy. Here, we provide the first demonstration of efficient and stable full-cycle redox transformations, synthesizing solar chemicals.

The identification of a successful redox cycle ensued from fluorescent quenching screening, which bridges between optoelectronic material properties and photosynthetic activity. Implementing this approach on hybrid nanorod photocatalysts (CdSe@CdS-Pt), we demonstrate hydrogen production with photon to hydrogen quantum efficiencies of up to ~70%, under visible light and mild conditions, while simultaneously harvesting solar chemical potential for valuable oxidative chemistries. Facile spectrophotometric analyses further show robust photo-chemical and colloidal stability, as well as product selectivity when converting molecules carrying amino- and alcohol-groups, with solar-to-chemical energy conversion efficiencies of up to 4.2%. As such, rigorous spectroscopic assessment and operando characterization yield superior photosynthetic performance, realizing a truly light-triggered catalytic reaction and establishing nanostructured metal-chalcogenide semiconductors as state-of-the-art artificial photo-chemical devices.

Key words: Homogenous photocatalysis; Solar chemistry; Hybrid nanorods; Artificial photosynthesis; Water splitting; Benzylamine oxidation.

TOC Figure

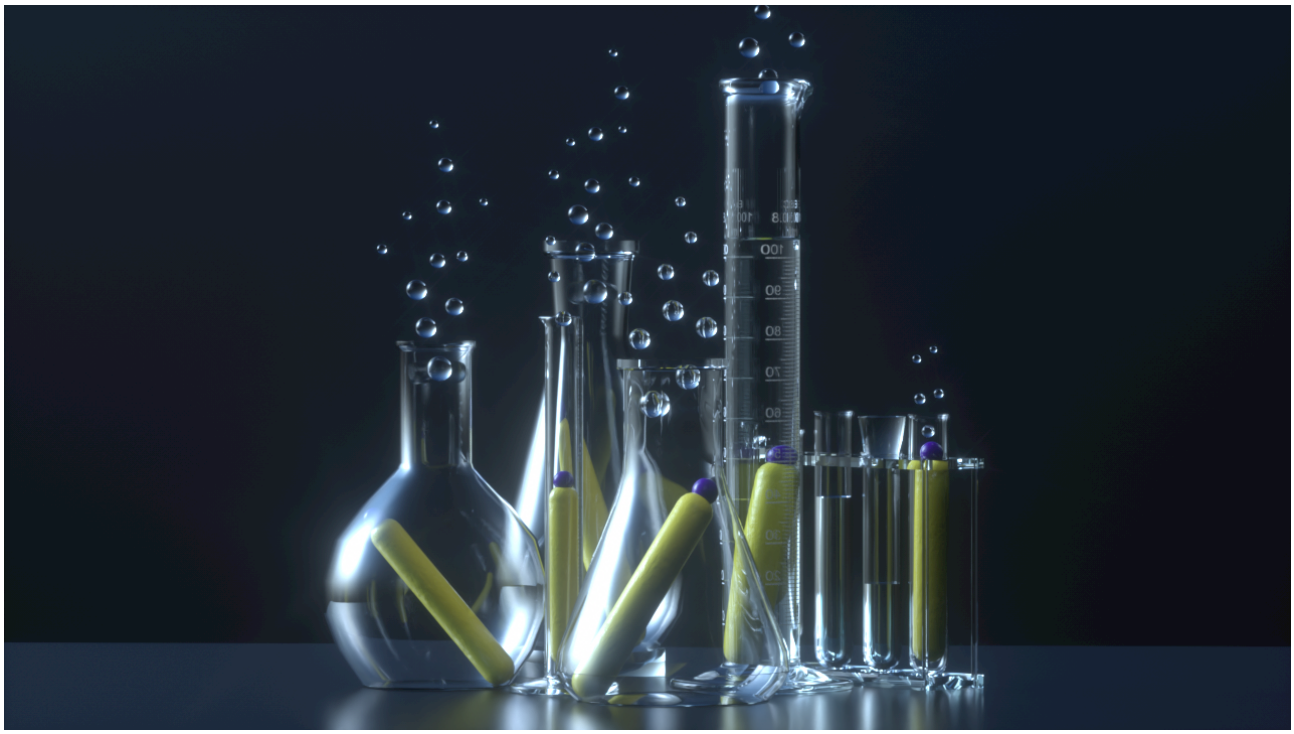

Towards Solar Factories, following Ciamician's Dream (Science, 1912): "*Forests of glass tubes will extend over the plains and glass buildings will extend everywhere; inside of these will take place the photochemical processes that hitherto have been the guarded secret of the plants"*

1. Introduction

A recent report from the *Intergovernmental Panel on Climate Change* (IPCC) called for immediate and prompt actions against anthropogenic-derived climate changes, compelling policymakers to the ultimate need of limiting global warming to 1.5°C[1]. In sight of this ambitious and mandatory goal, effective technological solutions in solar energy harvesting and accumulation are required in the imminent future. Photocatalytic water-splitting is, to this extent, one the most promising, yet developing strategy to directly convert solar irradiation to chemical energy[2–7]. This process can generate, in mild conditions, a high gravimetric energy-dense fuel like hydrogen, and oxygen as by-product. While the former is a highly demanded commodity in the energy, semiconductor and agricultural sectors, oxygen production is industrially performed by distillation of air and is less attractive under both technological and economical point of view when obtained by electrolysis of water. First, simultaneous hydrogen (H_2) and oxygen (O_2) generation poses safety risks in the reactor design, and increases its cost due to the need for a gas separation system[8,9]. Moreover, besides having low value as a chemical commodity, O_2 synthesis introduces severe kinetic and durability limitations on the reaction performance, representing in fact the bottleneck of the whole process[10,11]. Consequently, state-of-the art efficiencies for overall photocatalytic water splitting do not exceed 2%[12]. Therefore, alternative oxidative pathways that could boost the market value of solar-to-fuel conversion have been recently proposed[13]. Among these, organic transformations and photo-reforming have been successfully demonstrated to simultaneously proceed along with molecular hydrogen production[14–16]. These processes aim at synthesising pharmaceuticals, fine-chemicals and value-added products from readily oxidised species, or alternatively decomposing underutilized or even harmful products found at large-scale in the environment[17]. Notably, alternative oxidative routes, which decouple H_2 production from O_2 evolution, are beneficial to photocatalysis, with the clear advantage of product formation in different phases, along with potentially prolonged catalyst stability. While such application in electrochemistry has gained broad attention over the last decade, photocatalytic demonstrations of such processes are lagging behind[18,19].

Cadmium sulfide (CdS) is among the few materials with suitable band gap to support water splitting, but it is hampered by photochemical instability[20]. Hence, CdS based photocatalysts are expected to greatly benefit from such coupling with alternative organic oxidative reactions. Most recently platinum-tipped CdS nanorods functionalized with a molecular Ru(tpy)(bpy)Cl_2-based oxidation catalyst were reported to support overall water splitting[21]. Despite the scientific achievement, O_2 was not produced with stoichiometric ratio, the quantum yield of the process was limited to 0.1-0.27%, and the system lost its activity after only 1-2 hours of operation. In contrast,

the closely related system composed of Pt-tipped CdS rod with an embedded CdSe seed demonstrated record activity towards the photocatalytic water reduction half-reaction, with a perfect 100% photon-to-hydrogen conversion efficiency, and long term stability, pending on replenishment of hole scavengers[22]. These highlight the enormous performance gap separating the two distinct half-reactions. Notably, fast oxidation kinetics can prevent hole accumulation in the light-absorber, surpassing the fundamental photo-corrosion phenomena that limits the performance of metal chalcogenide based photocatalyst[23,24]. As a result, finding alternative processes to efficiently harvest the chemical potential of positive photo-generated charge carriers represents an opportunity and an urgent need at the same time[25].

Here, we present an impressive 69% photon-to-hydrogen conversion efficiency (with ~43% under monochromatic irradiation at 455nm) that are obtained from Pt-tipped CdSe@CdS rods, under visible light excitation, at room temperature, and in aqueous solution with neutral pH, along with simultaneous oxidation of benzylamine ($BnNH_2$). Rather than consuming sacrificial hole scavengers, we achieve a closed redox cycle with the simultaneous production of H_2 and selective synthesis of valuable benzaldehyde (industrially useful aromatic aldehyde, BnCHO) from both $BnNH_2$ and benzyl alcohol (BnOH). Remarkably, these endothermic reactions resulted in extensive utilization of solar chemical potential. Hence, this is a true photosynthetic system, rather than a photocatalytic one, which fosters only exothermic reactions[26]. We computed an impressive 4.2% solar-to-chemical energy conversion (STC). To this extent, we advance such performance metric as a fundamental gauge distinguishing light-harvesting strategies producing solar fuels, as attained in water splitting, from photosynthetic processes yielding a gallery of solar chemicals, along with H_2 generation.

Significantly, these specific oxidative reactions were selected by implementation of a unique screening method, based on fluorescence quenching, that is developed for fast, easy and rigorous assessment of potential candidate organic transformations. While exploration of better-suited oxidation reactions is gaining increased interest[27], keeping away from empiric trial-and-error approach will require the development of fast screening tools for high-throughput search[28]. Rigorous descriptors that can construct material-function correlation are expected to empower new computational techniques to classify photocatalyst suitability for specific purposes, eventually serving as fundamental driver for the whole interdisciplinary photocatalysis research community. To this extent, the formation of any light-triggered reactive species results from a general and inceptive optical event, i.e. the photo-induced electron transfer. Determining the efficiency of such process can, in particular, single-out suitable photo-oxidative organic reactions complementing the well-established hydrogen reduction counterpart. Preliminary thermodynamic considerations can further include a comparison between redox potentials of the photocatalyst excited state and

substrate ground state, according to the Gibbs free energy equation.[29] However, because of the irreversible nature of numerous chemical reactions, direct assessment of redox potential is experimentally inaccessible, complicating electron-transfer prediction in reaction-like conditions. While transient absorption spectroscopy gives access to kinetics behaviour, it requires complex and expensive instrumentations and difficult data analysis (in photoreaction conditions)[30,31]. As a result, we uniquely utilized steady-state and time-resolved photoluminescence quenching for mechanistic-based search of potential candidates for organic transformations[32]. Having ruled out energy transfer pathways, quenching of the light sensitizer component of the photocatalyst (i.e. CdSe@CdS rods) by organic electron-donors can be correlated to the number of holes extracted from the material and, accordingly, to the catalytic activity.

Overall, by means of readily accessible spectroscopic techniques, we capitalize on the excellent water reduction properties of a known photocatalyst, deploying its application to organic transformations, resulting in extensive solar energy conversion to (selective) imines or aldehydes chemical bonds alongside with H_2 fuel generation.

2. Results

2.1. Photoluminescence quenching investigation

Semiconductor based photosynthetic promotion of a redox reaction necessary involves charge or energy transfer from the photocatalyst to the molecule of interest. These processes are expected to inflict upon the level of photoluminescence quenching, which can thus serve as a simple inverse probe for the quality and quantity of such transfer[33].

In the course of this study we monitored photoluminescence quenching of CdSe@CdS dot-in-rod nanostructures (NRs). The rods were prepared as previously described[34]. The typical optical features of NRs, which are dispersed in toluene after synthesis, include an absorption edge at 460nm (attributed to the CdS shell), a weak absorption band at 570nm (attributed to CdSe core) and a strong emission centered at 575nm (as shown in Figure 1). Successive colloidal deposition of Pt nanoparticles on NRs apexes creates spatially separated redox centres, where the metal tip and CdSe quantum dot (QD) act, respectively, as electrons and holes sinks for photo-generated charge carriers, owing to the quasi-type II junction created by CdS and CdSe band alignment.[22] Metal tipped rods present negligible fluorescence emission of the ‘bare’ parent rods, indirectly suggesting successful capping of NRs by Pt nanoparticles, yet limiting further excited-state characterization. Thus, in order to investigate energy and/or electron-transfer phenomena occurring between the photocatalyst and different organic molecules, we employ bare NRs, rather than the full

photosynthetic system. The NRs represent an ideal platform for optical spectroscopic quenching studies, owing to their large molar extinction coefficient ($\varepsilon \sim 10^7$ $M^{-1}cm^{-1}$ at $\lambda = 400nm$) and high fluorescence quantum yield, typically around 40% (see supporting information Figure S1), that allows intense fluorescent signal detection with minimal sample utilisation (~10^{-7} mmol). Similarly, such outstanding optoelectronic properties allow for efficient light absorption at minimal concentration of sample suspended in solution (<10^{-5} % photocatalyst loading).

With the aim of coupling water reduction to electron-donor moieties oxidation, we study the interaction between NRs and two common organic substrates used in organic photoredox catalysis, namely benzylamine and benzyl alcohol. A preliminary screening has been performed by measuring the change of luminescence signal upon addition of the substrates to an aqueous solution of freshly prepared bare NRs. Quenching percentage is defined as $\% = \left(1 - I_{QUENCH}/I_0\right) \cdot 100\%$, where I_{QUENCH} and I_0 are the photoluminescence signals after addition of $BnNH_2$/BnOH and of bare NRs, respectively. All the quenching experiments have been performed holding constant absorbance at the excitation wavelengths ($A_{455} \sim 0.5$), and high substrate concentration regime (0.01 – 0.1 M), in order to assess their behaviour in photoreaction-like conditions. The absorption spectra of the mixtures are the mere superposition of the spectra of the rods and the quenchers: this indicates that the interaction between the two species is negligible at the ground state (see supporting information Figure S2). As expected, upon addition of $BnNH_2$ or BnOH, we observe fluorescence intensity decrease that is inversely proportional to the molecules' oxidation potential (+1.324V[35] and +1.98V vs NHE, respectively)[36]. Energy transfer quenching pathways can be ruled out, as the excited state of both quenchers lies at much higher energy compared to that of the NRs. In particular, in degassed water-acetonitrile (60/40) mixtures and substrate concentration of 0.05M, the presence of $BnNH_2$ reduced the NRs emission intensity by 44%, while the presence of BnOH resulted with merely 18% reduction of the emission intensity.

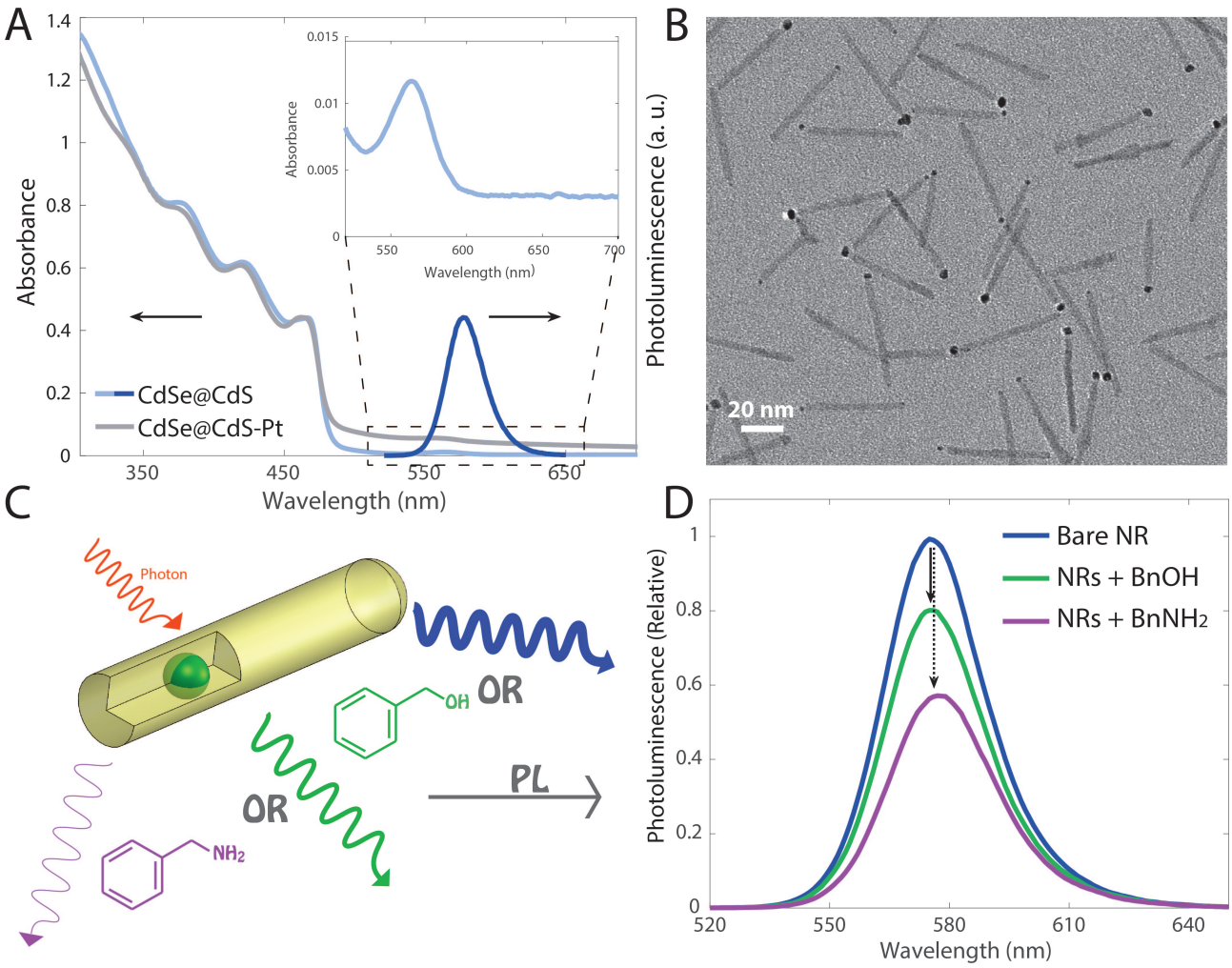

Figure 1. *(A) Absorption and emission spectra of CdSe@CdS and CdSe@CdS-Pt in water solution ([NRs] = 10^{-7} M, λ_{exc} = 455nm). The inset is a magnification of the absorption spectrum, showing the contribution of the CdSe QD. (B) Transmission Electron Microscopy image of CdSe@CdS-Pt NRs. (C) Schematic representation of the photoluminescence quenching experiment: after photoexcitation, the excited-state of bare NRs radiatively deactivates with high yield (blue curve) or undergoes hole transfer to BnOH (green curve) or $BnNH_2$ (violet curve) present in solution. In the latter cases, radiative deactivation occurs from a reduced population, the size being inversely proportional to the oxidation potential of quencher moieties. (D) Relative emission spectra of CdSe@CdS in water:acetonitrile (60/40) solution upon addition of 10^{-4} mol of BnOH (green line) and 10^{-4} mol of $BnNH_2$ (violet line).*

Motivated by the promising results, we investigate in more details the nature and the kinetics of the processes competing with radiative deactivation by Stern-Volmer analysis, based on emission intensities and excited-state lifetimes. Predictably, we obtain similar trends also in a more diluted substrate concentration interval (0.0001 - 0.001 M). We note that the excited-state depopulation dynamics is probably described by a combination of different quenching constants and multiple lifetimes, as evidenced by the presence of several linear slopes describing intensity of emission decay as a function of quencher concentration (supporting information Figure S3-4).

2.2. H_2 generation performance

Following photoluminescence quenching experiments, we investigate simultaneous water reduction and $BnNH_2$/BnOH oxidation, at room temperature and under neutral pH (Figure 2-3). Photosynthetic hydrogen production is evaluated under different experimental conditions and setups, proving inter-laboratory reproducibility and non-artificial figures of merit[37]. Typically, solutions of NRs and organic moieties were placed in a custom-built gas-tight reaction cell that is directly connected to a gas chromatograph equipped with a thermal conductivity detector and purged with argon. The solutions were then illuminated with a monochromatic light source (455 nm LED, adjusted to 50 mW; equivalent to a photon flux of $1.15 \cdot 10^{17} photons\ s^{-1}$). The evolving hydrogen was analyzed while operating in continuous flow mode, allowing for direct determination of the gas production rate. The apparent photon-to-hydrogen conversion efficiency of the sample, which is defined as the ratio between H_2 molecules produced and absorbed photons, $\mathrm{QE}_{PTH}(\%) = 2N_{H_2}/N_{hv} \cdot 100\%$, was determined by quantifying the amount of evolved hydrogen at a given photon flux. Notably, while toxic and non-innocent solvents are often used in the literature for improved solubility of the organic molecules, here we explored only mild experimental conditions, with water/organic solvent mixtures that were limited mostly to acetonitrile or ethanol[38]. In fact, whereas $BnNH_2$ oxidation necessarily requires the use of an organic solvent, with a water-acetonitrile (60/40) mixture outperforming more diluted ratios or water-ethanol mixtures, BnOH appears to be sufficiently soluble in pure water.

Under continuous monochromatic irradiation, simultaneous H_2 generation and $BnNH_2$ oxidation demonstrates performances in agreement with the high sensitivity of the NRs to the substrate, as evidenced by fluorescence quenching. Following rapid purging with Ar (10-20 minutes), the reactions proceed for nearly 10 hours reaching a maximum QE_{PTH} of 37% (Figure 2A). Remarkably, once maximal H_2 production rate is attained, it persists for about an hour before decreasing as a result of diminishing concentration of $BnNH_2$ (see reaction scheme Figure 5). The performance time trajectories of Pt tipped CdSe@CdS NR photocatalysts are known to display an induction time until full activity is reached[34]. One possible explanation for the induction time is reorganization of the ligands on the photocatalysts surface. Here, it is clear that the $BnNH_2$ concentration started to diminish long before the end of such induction period, and before the NR photocatalyst attained its optimal performance. Upon replenishment of electron donor via subsequent injections of fresh reagent ($BnNH_2$), as soon as noticeable decrease in QE_{PTH} is detected, H_2 production restores, and the photosynthetic activity improves further. Specifically, this results in the achievement of nearly ~43% photon-to-hydrogen conversion efficiency, with a turn over

frequency of ~300,000 H_2 molecules per rod per hour, and a total production of 1.48 mmol of H_2 in 16 hours of irradiation.

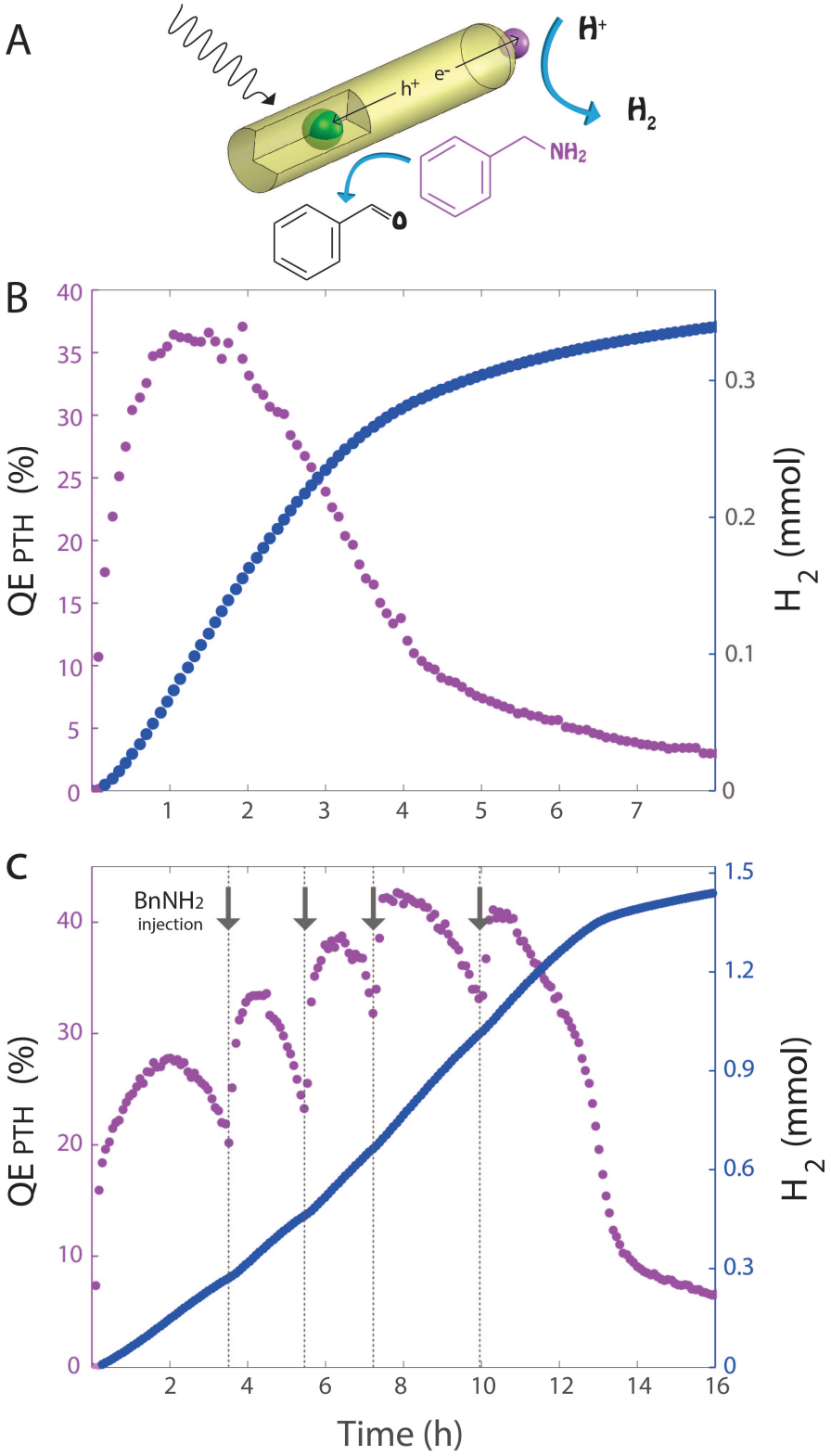

Figure 2. *(A) Schematic representation of the simultaneous photosynthetic H_2 production and $BnNH_2$ oxidation. Reactions are performed both without (B) and with (C) addition of fresh reagent during the irradiation. Left y-axes refer to photon-to-hydrogen quantum efficiency violet curves), while right y-axes refer to the total H_2 moles produced (blue curves). Experimental conditions used:* $[BnNH_2]_{t=0} = 0.05\ (M)$*, [Pt-NRs] = $3.5 \cdot 10^{-8}$ M with catalyst loading = $7 \cdot 10^{-5}$ %, reaction volume = 10 mL, light source: 455nm LED (50mW), T = 25°C, solvent: H_2O/CH_3CN (60/40).*

It is reasonable to believe that accumulation of oxidative product in the reaction cell over time is detrimental to the photocatalyst activity. Hence, we expect that operation in flow conditions that would enable both constant replenishment of $BnNH_2$ and clearance of the product, would result with future improvement in catalytic activity and reaction yield.

Upon coupling H_2 generation to oxidation of BnOH, the photosynthetic yields dropped, as anticipated by fluorescence quenching analysis. The photon-to-hydrogen conversion efficiency was only slightly affected by the solvent, with QE_{PTH} of 9.4% obtained from water-acetonitrile mixture, and 7.3% for pure water (Figure 3). For these reactions, we report turn over frequency of ~71,000, and ~58,000 H_2 molecules per rod per hour, respectively.

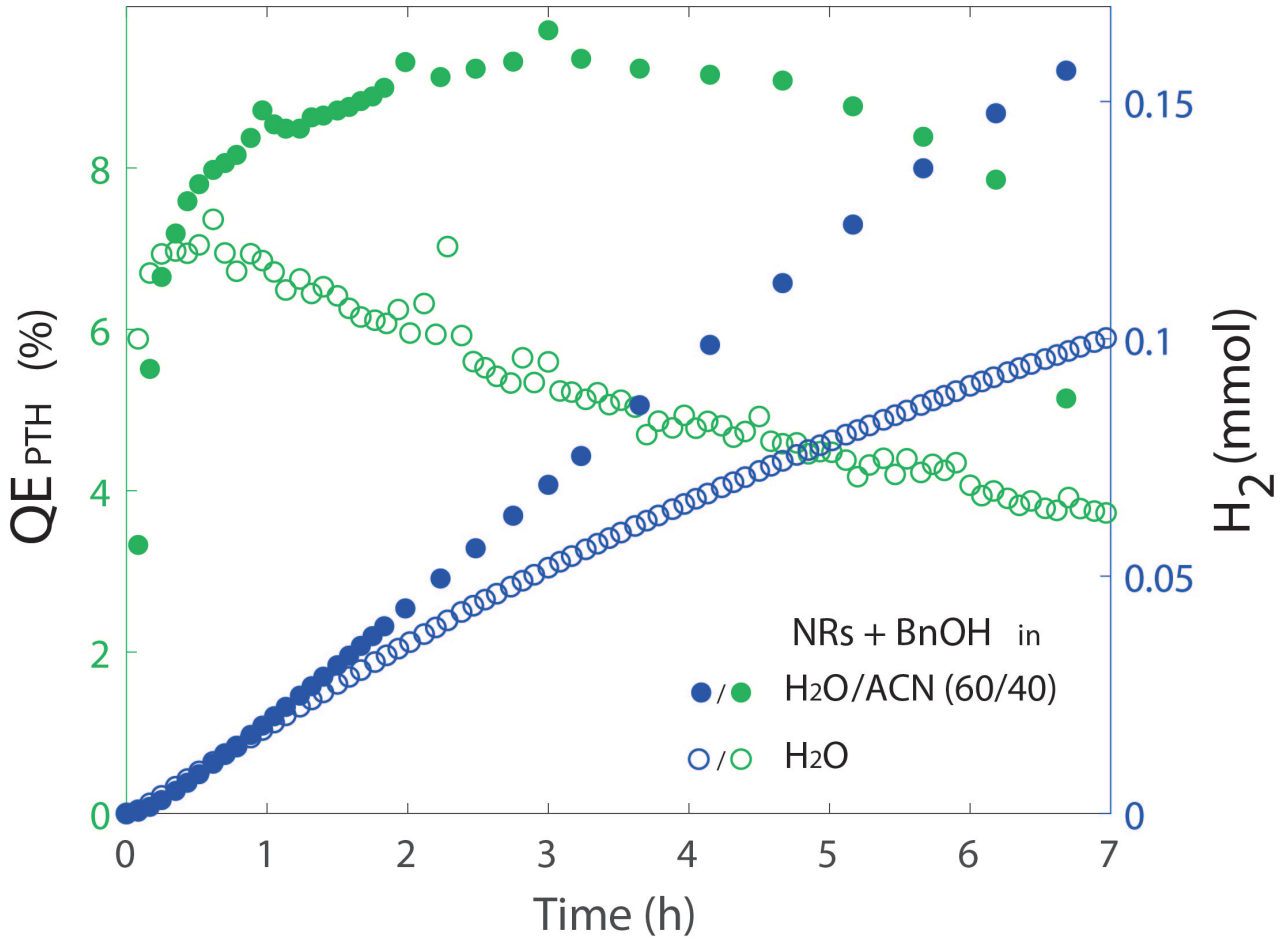

Figure 3. *Simultaneous photosynthetic H_2 production and BnOH oxidation. Experimental conditions:* $[BnOH]_{t=0} = 0.05\ (M)$, *[Pt-NRs] = $3.5 \cdot 10^{-8}$ M with catalyst loading = $7 \cdot 10^{-5}$%, reaction volume = 10 mL, light source: 455nm LED (50mW), T = 25 ºC, solvent: H_2O/ACN (60/40) (filled dots) and H_2O (empty dots). Left y-axis refers to photon-to-hydrogen quantum efficiency (green dots), while right y-axis refers to total H_2 moles produced (blue dots).*

Since the overall closed redox cycle promoted endothermic reactions, the solar energy was harnessed and converted into chemical potential. In order to estimate the energy conversion efficiency, photosynthetic measurements were performed in the same conditions under simulated solar sunlight (0.1 sun), using a long-pass filter (λ > 400nm). The H_2 generation performance

recorded over the course of 50 hours is presented in Figure 4. Under these conditions, photon-to-hydrogen conversion efficiency was calculated by computation of the photon flux absorbed by NRs under this polychromatic irradiation (dark gray trace in the inset of Figure 4, see Supporting Information for detailed calculations), and a maximum QE_{PTH} of 69% was obtained (Figure 4, violet). We speculate that operation under polychromatic excitation lifts absorption-saturation limitations, contributing to the improved efficiency compared with monochromatic irradiation at 455nm. In addition, the $BnNH_2$ concentration was doubled in order to extend the active operation time, leading to faster holes scavenging and, consequently, to an increase of QE_{PTH}.

In order to assess the extent of solar chemical potential that has been harvested through the photosynthetic reaction, we computed the process efficiency according to solar-to-chemical (STC) definition, i.e. $\eta_{STC}\ (\%) = (J_{rxn} \cdot \mu_{rxn})/(P_{Solar} \cdot \mathrm{A}) \cdot 100\%$, where $J_{rxn}$and μ_{rxn} are the rate and chemical potential of the reaction performed, P_{Solar} the total incoming power and A the irradiated area. Noticeably, the chemical potential is defined as the partial molar Gibbs free energy (ΔG) of the synthesised photoproducts. The results are presented in Figure 4 in blue. During optimal performance, the H_2 production rate (J_{rxn}) was 0.01 $mmol\ h^{-1}$, while total incident power at the solution surface amounted to $22.4\ mW$ (0.1 sun, $80\ J\ h^{-1}$). Overall, considering an endothermic barrier of $335.4\ kJ\ mol^{-1}$ (μ_{rxn}) that is needed to simultaneously reduce H^+ and oxidize $BnNH_2$, the photosynthetic performance reached a maximum of 4.2% STC efficiency (See SI for detailed calculations). When considering the STH index as the STC efficiency for the water splitting reaction ($\mu_{rxn} = 237\ kJ\ mol^{-1}$), it is possible to notice that the performance obtained largely surpasses the best state-of-the-art efficiency for hydrogen generation via suspended photocatalysts[39].

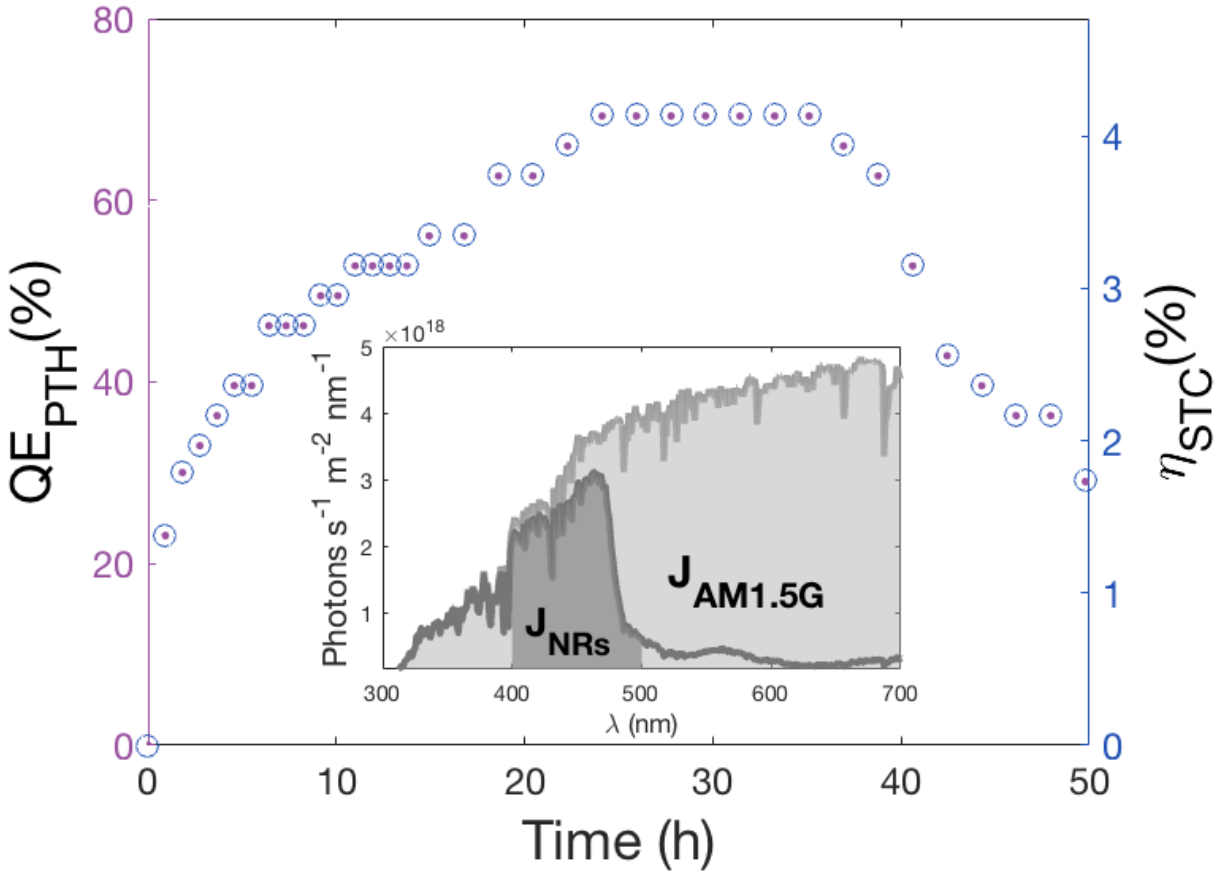

Figure 4. *Simultaneous photosynthetic H_2 production and $BnNH_2$ oxidation. Experimental conditions:* $[BnNH_2]_{t=0} = 0.1(M)$*, [Pt-NRs] = 3.5·10^{-8} M with catalyst loading = 3.5·10^{-5} %, reaction volume = 10 mL, light source: AM1.5G (0.1 sun) solar-simulator fractioned with a 400nm long-pass filter, T = 25°C, solvent: H_2O/CH_3CN (60/40). Left y-axis refers to photon-to-hydrogen quantum efficiency (violet dots), right y-axis refers to solar-to-chemical (blue circles). Inset: AM1.5G photons flux (light gray curve) superimposed to the scaled photons flux absorbed by NRs (dark gray curve). Dark gray area indicates the fraction of light included between long-pass filter and QD valence band.*

Finally, control experiments show that no H_2 is produced in the absence of CdSe@CdS-Pt NR photocatalysts, light or electron-donor moieties (see supporting information Figure S7).

2.3.Materials Photo-stability and Reaction Selectivity

As demonstrated in Figures 2B and 4, Pt-tipped CdSe@CdS NRs exhibit long-term stability, as long as the $BnNH_2$ electron donor is replenished. Aliquots of the reaction mixture were analysed throughout irradiation, limiting the extraction to small volumes (~50µL) in order to only negligibly affect the photoreactor's optical path length and amount of active sample in the reactor. Figure 6A displays an example of absorbance trace development throughout irradiation. The unaltered NRs quantum features and baseline scattering clearly demonstrate that the photocatalyst does not undergo degradation nor particle aggregation in the time window during which oxidative reactions are completed.

The products from the organic transformations were investigated by means of gas chromatography mass spectrometry (GC-MS), thin-layer chromatography (TLC) and, provided the photocatalyst robustness with respect to the investigated organic transformations, also by UV-Vis spectroscopy. In accordance with previously proposed light-triggered oxidative mechanisms carried out in similar experimental conditions[36,38,40], we first selectively convert $BnNH_2$ into benzylidenebenzylamine. After that, the presence of water promotes hydrolysis of the so formed imine to the related benzaldehyde and benzylamine (Scheme in Figure 5). Continuous irradiation leads to further oxidation of the newly formed $BnNH_2$, shifting the latter reaction out of equilibrium towards the accumulation of benzaldehyde, as shown by GC-MS signal evolution (see Figure 5C). For the first part of the reaction, two molecules of $BnNH_2$ react to form the imine for every H_2 molecule formed, corroborating the complete consumption of the initial 0.525 mmol of amine after 3 hours (see Figure 2A). A complete balance of the overall reaction finally suggests that, for the consumption of one molecule of $BnNH_2$, one molecule of benzaldehyde and one of H_2 are produced, decreasing by 50% the consumption of $BnNH_2$ per H_2.

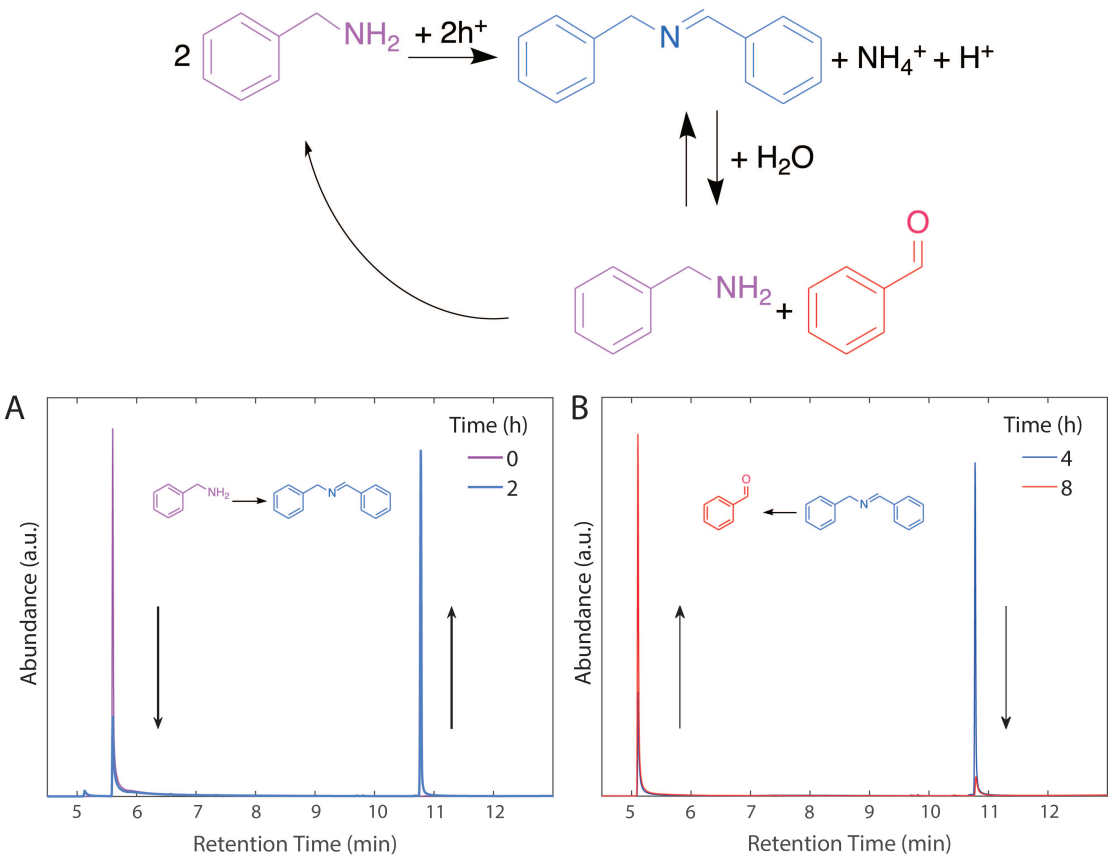

Figure 5. *Mechanism of anaerobic $BnNH_2$ photo-oxidation, occurring with simultaneous H^+ photo-reduction. The upper panel exhibits a schematic representation of the organic transformation in accordance to GC-MS analysis. GC-MS data – presented in panels 5A and 5B – refer to the analysis of reaction aliquots extracted after 0, 2, 4 and 8 hours of irradiation. Initially, $BnNH_2$ (violet trace) selectively converts to N-benzylidenebenzylamine (blue trace), that in turns hydrolises to $BnNH_2$ and BnCHO (green trace) in the H_2O-CH_3CN mixture. The recurring formation of $BnNH_2$ proceeds therefore until its complete conversion to BnCHO.*

In general, in-operando analysis of the reaction mixture can reveal problematic. Traditional NMR product investigation may, at times, be insufficiently sensitive for the analysis of small volumes or low conversion yields. Here, in light of the photocatalyst robustness, we unravel product analysis for BnOH oxidation by UV-Vis absorption spectroscopy, owing to the technique's high sensitivity. Specifically, we demonstrate that oxidation product can be easily detected even from highly diluted reaction fractions, via monitoring typical absorption characteristics in the UV part of the spectrum. This is shown here for the oxidation of BnOH in Figure 6B. The mechanism for photosynthetic oxidation of BnOH was found to be analogous to the anaerobic electrochemical oxidation of the same compound, in which two electrons and two protons are extracted to form the benzaldehyde (BnCHO).[41] Consequently, the production of one H_2 molecule corresponds to the synthesis of one BnCHO molecule. Before irradiation, the BnOH trace sits above NRs absorbance with a distinct feature peaking at ~260nm. With time progression, two features evolve at ~290 and ~250nm, perfectly overlapping a reference benzaldehyde absorbance spectrum, superimposed in black to the trace referring to t = 8 hours in Figure 6B (light-green curve). Notably, the characteristic absorbance peak below 250 nm[42] that correlate with formation of benzoic acid was not observed. In accordance to subsequent GC-MS analysis (see supporting information Figure S8), we therefore demonstrate selective conversion of benzyl alcohol to benzaldehyde, without detectable formation of benzoic acid.

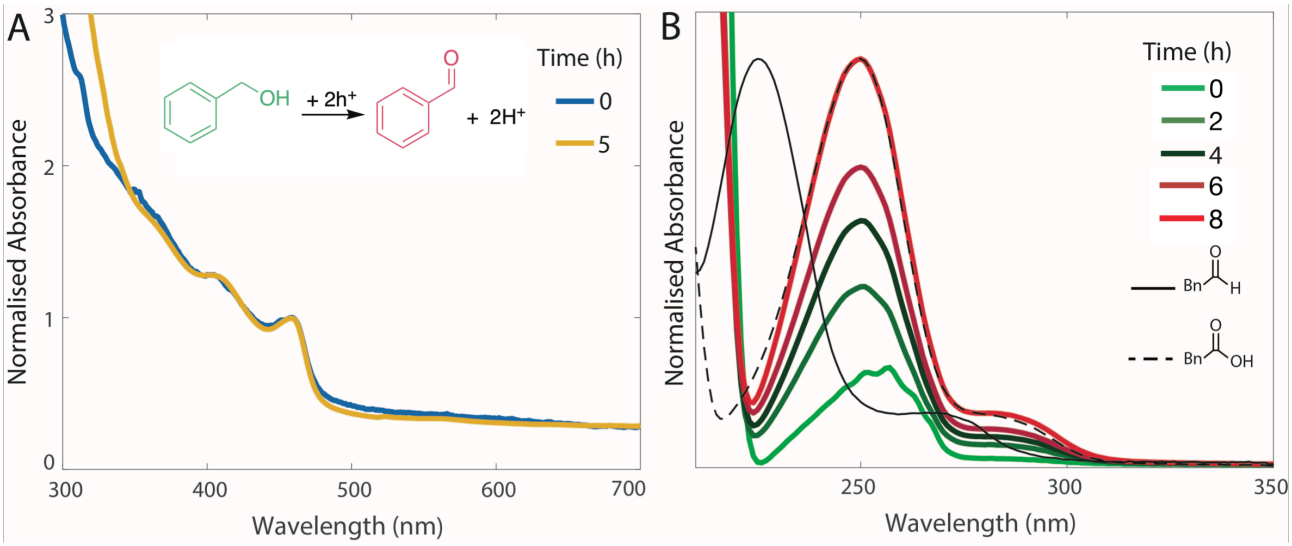

Figure 6. *Spectrophotometric analyses of crude reaction mixtures. Panel A highlights the photocatalyst stability as evident by absorbance trace before and after 5h of irradiation. Panel B displays evidence for reagent and product traces, sitting on top of Pt-NRs absorbance in the UV region. Reference absorption spectra of benzaldehyde (BnCHO, dashed balck line) and benzoic-acid (BnCOOH, solid black line) have been added for convenience. Curves in both plots are normalized to NRs first absorption peak.*

3. Discussion

Despite the potential of being techno-economically more attractive than photo-electrocatalysis,[43] particle-based photocatalysis often suffers from fundamental applicative limitations. System photo-stability and lack of reaction selectivity are especially relevant in this sense. Here we endeavor to both shortcomings.

First, fluorescence emission quenching was established as an invaluable platform to evaluate value-added chemicals for decoupled water reduction and oxidation reactions. Owing to rapid and accessible experimental requirements of this method, we promptly assessed photoinduced electron-transfer interaction between CdSe@CdS NRs and two appealing substrates used in oxidative organic transformations. Taking advantage of the excellent water reduction capability of metal tipped dot-in-rod photocatalysts, we therefore aimed at realizing a highly efficient and closed redox cycle, irrevocably surpassing sacrificial charge-carriers harvesting. Secondly, we provided initial evidence of novel photophysical phenomena occurring at the nanostructure-solvent interface. By thoroughly investigating excited-state dynamics by fluorescence experiments, we indeed discovered the presence of a concentration dependent regime of luminescence quenching. We speculate that the fluctuating nature of ligand density coverage of the nanostructure surface plays a non-negligible role. In particular, it prevents us from clearly distinguishing between static and/or dynamic quenching. Such description is further complicated by the nature and role of the multiple exponential components characterizing emission lifetimes. We expect that more detailed kinetics investigation with complementary optical techniques will guide us in the definition of optimal post-synthetic protocols for ad-hoc photosynthetic application.

Since photo-corrosion represents the primary Achilles tendon of metal-chalcogenide photocatalysts, finding effective hole-removal strategies is, therefore, of crucial importance. Fluorescence spectroscopy directly targets these issues, and we prove that both $BnNH_2$ and BnOH oxidation proceeds with high turnover, without compromising NRs durability. Such results stand as an excellent advancement in the field, since chemical and colloidal instabilities are long-standing plagues for metal-chalcogenide and nanostructured suspended photocatalysts, respectively[23]. Concerning the latter deactivation mechanism, recent reports have proposed “ligand-free” nanosystem configurations[16], however we corroborate their passivation function to be indispensable for long-term photosynthetic experiments. To this extent, we estimated a turnover of ~10^6 H_2 molecules per NR during the 18 hours-long continuous benzylamine oxidation (Figure 2C). The concomitant demonstration of material's stability and excellent QE_{PTH}/STC throughout such long-standing irradiation (Figures 2C and 4) further implies the prospect of higher reaction turnovers.

Finally, we regard the present work as a major endeavor to realize a highly efficient artificial photosynthetic system for the forthcoming solar-industrial age[44,45]. In particular, water reduction displays comparable performances with respect to recent photocatalytic demonstrations that take advantage of sacrificial hole-scavengers. State-of-the-art ZnS NRs photocatalyst employed for combined H_2 production and ascorbic acid oxidation indeed yielded 149 $mmol_{H2}$ $g^{-1}h^{-1}$[46], while we obtain 181 $mmol_{H_2}$ $g^{-1}h^{-1}$. Considering instead relevant chemical transformation that avoid sacrificial substrates, we demonstrate, in milder experimental conditions, oxidative reactions with rates several orders of magnitude higher compared to similar N-benzylidenebenzylamine and benzaldehyde formation[14,38]. For this specific case, we also proved that multiple additions of the starting reagent increased the efficiency even further. We attribute this behaviour to diffusion-limited access of the photocatalyst to target substrate for the oxidation reaction, namely $BnNH_2$ and BnOH. By replenishment of such substrates in solution at complete conversion of the initial amount, efficiency rises again because of the presence of electron-donors that outcompete alternative hole-transfer pathways. In light of this, we envisage that faster mass-transfer characteristics provided by flow-photoreactors will relax such obstacles, potentially resulting in higher yields, reduced reactions times and eventually industrially scalable process conditions[47].

Overall, hybrid CdSe@CdS-Pt NRs are established as a perfect platform to extend the use of fluorescence quenching to other value-added reactions of industrial importance, coupled to efficient simultaneous H_2 generation. Future work will strive to incorporate more abundant and non-toxic materials for the photocatalytic system, in lieu of this Cd based structure.

4. Conclusion

We demonstrated a spectroscopic protocol to predict and analyse suitable organic transformations to be coupled to photosynthetic H_2 generation. Using hybrid CdSe@CdS-Pt nanorods, a maximum turn over frequency of ~300,000 H_2 molecules per rod per hour was obtained, with maximum STC and PTH efficiencies of 4.2% and 69%, respectively, while maintaining unaltered chemical and colloidal properties. Selective reaction pathways were demonstrated via GC-MS and UV-Vis absorption spectroscopy for $BnNH_2$ and BnOH oxidation. Moreover, we anticipate the possibility to relax current limitations and further increase reaction yields by application of flow conditions.

Acknowledgments

We gratefully acknowledge the H2020-MSCA-ITN-2016 (722591- PHOTOTRAIN), and the support of the Israeli Ministry of National Infrastructures, Energy and Water Resources (grant number 218-11-044). This research was partially carried out in the framework of the Russell Berrie Nanotechnology Institute (RBNI) and the Nancy and Stephen Grand Technion Energy Program (GTEP).

References

[1] Intergovernamental Panel on Climate Change, Global Warming Of 1.5 °C, 2018.
[2] Z. Zhigang, Y. Jinhua, S. Kazuhiro, A. Hironori, Direct splitting of water under visible light irradiation with an oxide semiconductor photocatalyst., Nature. 414 (2001) 625–627.
[3] A. Kudo, Y. Miseki, Heterogeneous photocatalyst materials for water splitting, Chem. Soc. Rev. 38 (2009) 253–278.
[4] X. Chen, S. Shen, L. Guo, S.S. Mao, Semiconductor-based photocatalytic hydrogen generation, Chem. Rev. 110 (2010) 6503–6570.
[5] R. Abe, Recent progress on photocatalytic and photoelectrochemical water splitting under visible light irradiation, J. Photochem. Photobiol. C Photochem. Rev. 11 (2010) 179–209.
[6] S.Y. Reece, J.A. Hamel, K. Sung, T.D. Jarvi, A.J. Esswein, J.J.H. Pijpers, D.G. Nocera, Wireless solar water splitting using silicon-based semiconductors and earth-abundant catalysts, Science. 334 (2011) 645–648.
[7] Y. Tachibana, L. Vayssieres, J.R. Durrant, Artificial photosynthesis for solar water-splitting, Nat. Photonics. 6 (2012) 511–518.
[8] S. Haussener, C. Xiang, J.M. Spurgeon, S. Ardo, N.S. Lewis, A.Z. Weber, Modeling, simulation, and design criteria for photoelectrochemical water-splitting systems, Energy Environ. Sci. 5 (2012) 9922–9935.
[9] D.M. Fabian, S. Hu, N. Singh, F.A. Houle, T. Hisatomi, K. Domen, F.E. Osterloh, S. Ardo, Particle suspension reactors and materials for solar-driven water splitting, Energy Environ. Sci. 8 (2015) 2825–2850.
[10] J. Tang, J.R. Durrant, D.R. Klug, Mechanism of photocatalytic water splitting in TiO_2. Reaction of water with photoholes, importance of charge carrier dynamics, and evidence for four-hole chemistry, J. Am. Chem. Soc. 130 (2008) 13885–13891.
[11] K.S. Joya, Y.F. Joya, K. Ocakoglu, R. van de Krol, Water-splitting catalysis and solar fuel devices: artificial leaves on the move, Angew. Chemie Int. Ed. 52 (2013) 10426–10437.
[12] J. Liu, Y. Liu, N. Liu, Y. Han, X. Zhang, H. Huang, Y. Lifshitz, S.-T. Lee, J. Zhong, Z. Kang, Metal-free efficient photocatalyst for stable visible water splitting via a two-electron pathway, Science. 347 (2015) 970–974.
[13] E. Reisner, When does organic photoredox catalysis meet artificial photosynthesis?, Angew. Chemie Int. Ed. 58 (2019) 3656–3657.
[14] H. Kasap, C.A. Caputo, B.C. Martindale, R. Godin, V. Wing-hei Lau, B. V. Lotsch, J.R. Durrant, E. Reisner, Solar-driven reduction of aqueous protons coupled to selective alcohol oxidation with a carbon nitride−molecular Ni catalyst system, J. Am. Chem. Soc. 138 (2016) 9183–9192.
[15] T. Uekert, M.F. Kuehnel, D.W. Wakerley, E. Reisner, Plastic waste as a feedstock for solar-

driven H_2 generation, Energy Environ. Sci. 11 (2018) 2853–2857.
[16] D.W. Wakerley, M.F. Kuehnel, K.L. Orchard, K.H. Ly, T.E. Rosser, E. Reisner, Solar-driven reforming of lignocellulose to H_2 with a CdS/CdOx photocatalyst, Nat. Energy. 2 (2017) 17021–17030.
[17] A. V. Puga, Photocatalytic production of hydrogen from biomass-derived feedstocks, Coord. Chem. Rev. 315 (2016) 1–66.
[18] B. You, G. Han, Y. Sun, Electrocatalytic and photocatalytic hydrogen evolution integrated with organic oxidation, Chem. Commun. 54 (2018) 5943–5955.
[19] S. Caramori, F. Ronconi, R. Argazzi, S. Carli, R. Boaretto, E. Busatto, C.A. Bignozzi, Solar energy conversion in photoelectrochemical systems, in: Appl. Photochem., Springer, Cham, 2016: pp. 67–143.
[20] K. Wu, T. Lian, Quantum confined colloidal nanorod heterostructures for solar-to-fuel conversion, Chem. Soc. Rev. 45 (2016) 3759–4034.
[21] C. Wolff, P. Frischmann, M. Schulze, B. Bohn, R. Wein, P. Livadas, M. Carlson, F. Jäckel, J. Feldmann, F. Würthner, J.K. Stolarczyk, All-in-one visible-light-driven water splitting by combining nanoparticulate and molecular co-catalysts on CdS nanorods, Nat. Energy. 3 (2018) 862–869.
[22] P. Kalisman, Y. Nakibli, L. Amirav, Perfect photon-to-hydrogen conversion efficiency, Nano Lett. 16 (2016) 1776–1781.
[23] P. V. Kamat, J.A. Christians, J.G. Radich, Quantum dot solar cells: hole transfer as a limiting factor in boosting the photoconversion efficiency, Langmuir. 30 (2014) 5716–5725.
[24] H. Kisch, Semiconductor photocatalysis for chemoselective radical coupling reactions, Acc. Chem. Res. 50 (2017) 1002–1010.
[25] K.P. Acharya, R.S. Khnayzer, T. O'Connor, G. Diederich, M. Kirsanova, A. Klinkova, D. Roth, E. Kinder, M. Imboden, M. Zamkov, The role of hole localization in sacrificial hydrogen production by semiconductor–metal heterostructured nanocrystals, Nano Lett. 11 (2011) 2919–2926.
[26] F.E. Osterloh, Photocatalysis versus Photosynthesis: A Sensitivity Analysis of Devices for Solar Energy Conversion and Chemical Transformations, ACS Energy Lett. 2 (2017) 445–453.
[27] P. Kalisman, Y. Kauffmann, L. Amirav, Photochemical oxidation on nanorod photocatalysts, J. Mater. Chem. A. 3 (2015) 3261–3265.
[28] C. Draxl, M. Scheffler, NOMAD: The FAIR concept for big data-driven materials science, MRS Bull. 43 (2018) 676–682.
[29] V. Balzani, G. Bergamini, P. Ceroni, Light: a very peculiar reactant and product, Angew. Chemie Int. Ed. 54 (2015) 11320–11337.
[30] J.K. Utterback, A.N. Grennell, M.B. Wilker, O.M. Pearce, J.D. Eaves, G. Dukovic, Observation of trapped-hole diffusion on the surfaces of CdS nanorods, Nat. Chem. 8 (2016) 1061–1066.
[31] K. Wu, Y. Du, H. Tang, Z. Chen, T. Lian, Efficient Extraction of Trapped Holes from Colloidal CdS Nanorods, J. Am. Chem. Soc. 137 (2015) 10224–10230.
[32] M.N. Hopkinson, A. Gómez-Suárez, M. Teders, B. Sahoo, F. Glorius, Accelerated discovery in photocatalysis using a mechanism-based screening method, Angew. Chemie Int. Ed. 128 (2016) 4434–4439.
[33] M. Marchini, G. Bergamini, P.G. Cozzi, P. Ceroni, V. Balzani, Photoredox Catalysis: The Need to Elucidate the Photochemical Mechanism, Angew. Chemie Int. Ed. 56 (2017) 12820–12821.
[34] Y. Nakibli, L. Amirav, Selective Growth of Ni Tips on Nanorod Photocatalysts, Chem. Mater. 28 (2016) 4524–4527.
[35] Z.J. Wang, K. Garth, S. Ghasimi, K. Landfester, K.A.I. Zhang, Conjugated Microporous Poly(Benzochalcogenadiazole)s for Photocatalytic Oxidative Coupling of Amines under Visible Light, ChemSusChem. 8 (2015) 3459–3464.

[36] J.L. DiMeglio, B.M. Bartlett, Interplay of corrosion and photocatalysis during nonaqueous benzylamine oxidation on cadmium sulfide, Chem. Mater. 29 (2017) 7579–7586.
[37] L.Y. Kunz, B.T. Diroll, C.J. Wrasman, A.R. Riscoe, A. Majumdar, M. Cargnello, Artificial inflation of apparent photocatalytic activity induced by catalyst-mass-normalization and a method to fairly compare heterojunction systems, Energy Environ. Sci. 12 (2019) 1657–1667.
[38] H. Liu, C. Xu, D. Li, H.-L. Jiang, Photocatalytic hydrogen production coupled with selective benzylamine oxidation over MOF composites, Angew. Chemie Int. Ed. 57 (2018) 5379–5383.
[39] J.-W. Jang, J. Sung Lee, C. Soc Rev, J. Hyun Kim, D. Hansora, P. Sharma, Toward practical solar hydrogen production-an artificial photosynthetic leaf-to-farm challenge, Chem. Soc. Rev. 48 (2019) 1908–1971.
[40] R. Mazzaro, S. Boscolo Bibi, M. Natali, G. Bergamini, V. Morandi, P. Ceroni, A. Vomiero, Hematite nanostructures: An old material for a new story. Simultaneous photoelectrochemical oxidation of benzylamine and hydrogen production through Ti doping, Nano Energy. 61 (2019) 36–46.
[41] C.-C. Chang, L.-C.C. Chen, S.-J.L. Liu, Investigation of electro-oxidation of methanol and benzyl alcohol at boron-doped diamond electrode: evidence for the mechanism for fouling film formation, J. Phys. Chem. B. 110 (2006) 19426–19432.
[42] K. Kawamura, T. Yasuda, T. Hatanaka, K. Hamahiga, N. Matsuda, M. Ueshima, K. Nakai, Oxidation of aliphatic alcohols and benzyl alcohol by H_2O_2 under the hydrothermal conditions in the presence of solid-state catalysts using batch and flow reactors, Chem. Eng. J. 285 (2016) 49–56.
[43] F.E. Osterloh, Artificial photosynthesis with inorganic particles, in: Integr. Sol. Fuels Gener., 2018: pp. 214–280.
[44] G. Ciamician, The photochemistry of the future, Science. 36 (1912) 385–394.
[45] G.W. Brudvig, S. Campagna, Introduction to a themed issue of Chemical Society Reviews on artificial photosynthesis, Chem. Soc. Rev. 46 (2017) 6085–6087.
[46] M.F. Kuehnel, C.E. Creissen, C.D. Sahm, D. Wielend, A. Schlosser, K.L. Orchard, E. Reisner, ZnSe Nanorods as Visible-Light Absorbers for Photocatalytic and Photoelectrochemical H_2 Evolution in Water, Angew. Chemie Int. Ed. 58 (2019) 59–5063.
[47] D. Cambié, C. Bottecchia, N.J.W. Straathof, V. Hessel, T. Noël, Applications of continuous-flow photochemistry in organic synthesis, material science, and water treatment, Chem. Rev. 116 (2016) 10276–10341.